Time-Dependent Ultrastructural Changes to Porcine Stratum Corneum Following an Electric Pulse

Stephen A. Gallo, Arindam Sen, Mary L. Hensen, and Sek Wen Hui
Membrane Biophysics Laboratory, Roswell Park Cancer Institute, Buffalo, New York 14263 USA

ABSTRACT The morphological changes to heat-stripped porcine stratum corneum following an electroporating pulse were studied by time-resolved freeze fracture electron microscopy. Pulses at a supra-electroporation threshold of 80 volts and 300 μs were applied across the stratum corneum with a pair of copper plate electrodes, which also served as cooling contacts. Multilamellar vesicles of 0.1–5.5 mm in diameter in the intercellular lipid bilayers of the stratum corneum appeared in less than milliseconds after pulsing. Pulsed samples exhibited aggregations of vesicles, whereas only occasional single vesicles were seen in the unpulsed samples. Aggregates form in less than a millisecond and disappear within minutes after the pulse. Their size ranged from 0.3 to 700 mm^2. The size of individual vesicles, aggregate density, and size were analyzed as functions of postpulse time. These aggregate formations seem to be a secondary reaction to the pulse-induced skin permeabilization, determined by the resistance drop and recovery after the pulse. Heating the samples to 65°C also caused vesicle aggregates of similar appearance to form, suggesting that these aggregations are related to the heating effect of the pulse. Hydration is thought to play an important role in aggregate formation.

INTRODUCTION

The transdermal route for delivering drugs has potential advantages over other methods of delivery in terms of convenience, noninvasiveness, and reduction of drug degradation. The predominant barrier to transdermal drug delivery is the outermost layer of the skin, the stratum corneum (Hadgcraft and Guy, 1989; Bronaugh and Maibach, 1989). The stratum corneum is composed of several densely packed layers of flattened, dead, keratinized cells surrounded by lipid bilayers consisting primarily of ceramides, cholesterol, and free fatty acids (Madison et al., 1987; Hadgcraft and Guy, 1989; Schurer and Elias, 1992). The total thickness of the stratum corneum varies from 10 to 40 mm with an average thickness of 20 mm (Chizmadzhev et al., 1995; Bouwstra et al., 1995). This strongly hydrophobic environment inhibits molecular transit of hydrophilic particles, retarding evaporation of water from the inside and penetration of molecules from the outside. Disruption of this barrier is the key to successful transdermal delivery.

One method of reversibly disrupting the stratum corneum is through the application of short, high voltage electric pulses or electroporation. Electroporation has been used in vitro to permeabilize cells to enhance molecular delivery and transfection (Chang et al., 1992 and references therein). Short pulses (microsecond to millisecond) of pulse field strength sufficient to create a transmembrane potential of more than 0.5 volts cause the capacitive breakdown of the membrane dielectric, leading to transient permeability increases until the membrane recovers sometime after the pulse. Electrically, the skin can be modeled as a resistor and capacitor in parallel with most of the resistance residing in the stratum corneum (Yamamoto, 1977). Thus, if the skin were exposed to an electric pulse, most of the pulse voltage would fall across the stratum corneum, making it the site of the electroporation.

Several studies have observed the electrical properties of the skin during and after pulsing and found the resistance to decrease to 10% of its original value during pulse application and then to recover after the pulse, although sometimes slowly and incompletely. Extensive electrical characterizations have been made of the skin with respect to electroporation (Pliquett et al., 1995; Gallo et al., 1997). Molecular transport studies have also been conducted, and marked increases in calcein, methylene blue, and oligonucleotide flux have been observed across the stratum corneum with the application of electrical pulses (Prausnitz et al., 1993; Johnson et al., 1998; Zewert et al., 1995). Electrical parameters have been examined for their effect on transport (Bommannan et al., 1994; Vanbever and Preat, 1995; Johnson et al., 1998). These phenomena have been seen both in flow-through permeation chambers in which excised human stratum corneum is mounted, and in full thickness pig skin models. Similar flux increases have also been seen in vivo in hairless rats following pulse (Prausnitz et al., 1993).

Despite the wealth of data concerning skin electropermeabilization, its physical manifestation is not yet revealed. Theoretical models of the pulsed skin suggest that electropores are created in the lipid lamella and corneocyte membranes such that ions may flow straight through the stratum corneum (Chizmadhev et al., 1995). These electropores might be too small and too uncommon to be detected, being only a few nanometers in diameter and persisting only a few milliseconds. It has also been suggested that, at lower voltages, electroporation of appendageal linings of hair follicles and sweat glands occurs (Chizmadhev et al., 1998). Pliquett

Received for publication 3 August 1998 and in final form 27 January 1999.
Address reprint requests to Dr. Sek Wen Hui, Department of Molecular and Cellular Biophysics, Roswell Park Cancer Institute, Elm and Carlton Streets, Buffalo, NY 14263-0001. Tel.: 716-845-8595; Fax: 716-845-8683; E-mail: roswhui@acsu.buffalo.edu.

0006-3495/99/05/2824/09 $2.00

et al. (1996b) observed, through fluorescent microscopy, localized transport regions of dye on excised stratum corneum following high-voltage pulsing. These regions do not correspond to skin appendages but reach diameters of 40–80 mm and are only observed above a critical voltage. Unfortunately, the resolving power of fluorescence microscopy is not enough to reveal the intricate structural detail of these regions. Clearly, more data is needed before the mechanism can be elucidated.

Freeze-fracture electron microscopy is a powerful technique for examining the morphology of lipid structures with high resolution. A technique has been developed that uses rapid freezing followed by freeze-fracture electron microscopy to examine pulse-induced changes in the lipid lamella and cell membranes of stratum corneum in a time-dependent manner (Stenger and Hui, 1986; Chang and Reese, 1990; Van Hal et al., 1996). Pig skin, a good model for human skin with respect to the size and structure of the stratum corneum (Ferry et al., 1995), was heat-stripped for use in our experiments. We have examined the effect of an electric pulse on the morphology of the stratum corneum and the kinetics of morphological changes to better understand the fundamental mechanism behind electropermeabilization. This knowledge will help to further optimize the electrical parameters for possible use in transdermal and gene delivery in humans.

MATERIALS AND METHODS

Time-resolved freeze fracture electron microscopy (TFEM) was used to visualize porcine stratum corneum frozen immediately after the application of an electric pulse. The stratum corneum, obtained from a local abattoir or from experimental animals of Dr. John Canty (State University of New York, Buffalo, NY), was separated from the dermis and fat layer by heat stripping. A small piece of skin (e.g., 5 × 10 cm) was laid flat, wrapped in aluminum foil, and submersed in 65°C de-ionized water for 10 min. The stratum corneum was then carefully peeled from the underlying layer and stored in a cold room (4°C) in a desiccant jar for at least 24 h. Pieces of stratum corneum of 1.5 mm in diameter, slightly hydrated with filtered water, were sandwiched between two thin copper plate electrodes. The prepulse skin resistance ranged from 10^4 to 10^5 Ω cm^2. The distance between electrodes was kept constant using Mylar^{TM} spacers 25 μm thick. The electrodes were connected to a pulse generator (model 345; Velonex, Santa Clara, CA), which was triggered by an optical switch attached to the freezing plunger (Fig. 1). The sample, located at the end of the plunger, was pulsed at various times before it entered liquid propane, following the release of the spring-loaded plunger (Fig. 1). The pulse timing was accomplished through the time-of-flight as the trigger bar attached to the sample rod is propelled toward the liquid propane coolant container, passing through two optical switches. The first switch triggered the pulse generator and the second marked the precise time at which the sample was frozen. The outputs of both were recorded on an oscilloscope trace. The switches were optically triggered by fixed trigger bars connected to the plunger. The sample was pulsed at a voltage of 80 volts and a pulse length of 300 μs at set times of 0.5 ms, 12ms, 5 s, 60 s, and 300 s before freezing. The pulse generator (Model 345, Velonex) was used to produce square pulses, which were recorded on a digital storage oscilloscope (Fluke 99 Scopemeter Series II, Everett, WA). The resistivity of the stratum corneum during pulse was 10^2 to 10^3 Ω cm^2. The optical switches (Digikey Optical Sensor OR504-ND, Thief River Falls, MN) produce a 5-volt pulse that were used to trigger the pulse generator or to register the freezing time. For each time point, and also for the control, a data set of 7–8 repeat samples was collected.

Samples were also frozen after high-temperature exposure. A heat gun (Model HG 301 B, Master Appliance Corp., Racine, WI) was used to simulate the effects of pulse heating on the sample. The temperature at different distances from the heat gun was measured with a thermocouple. The temperatures were found to be stable (±1°C) and decreased proportionally with increasing distance. The sample was held ~30 cm in front of the gun. After the sample was heated for 15 s at 65°C, it was then hand plunged into liquid propane. A data set of six repeat samples was collected.

Samples were then fractured in a modified Polaron E-7700 unit at −115°C and 10^{-7} torr. Fracture planes were replicated by carbon/platinum and carbon evaporation at 45° and 90° to the fracture face, respectively, using Cressington ion guns (Fassel et al., 1991). Replicas were placed on copper grids (T400, Electron Microscopy Sciences, Fort Washington, PA) and examined in a Hitachi-600 electron microscope.

Each data point consisted of several repeat samples, incorporating skin from different regions of the body and separate animals. Each sample consisted of carbon/platinum replicas on several EM grids. The sampled replica area for each experiment was ascertained through light microscopy.

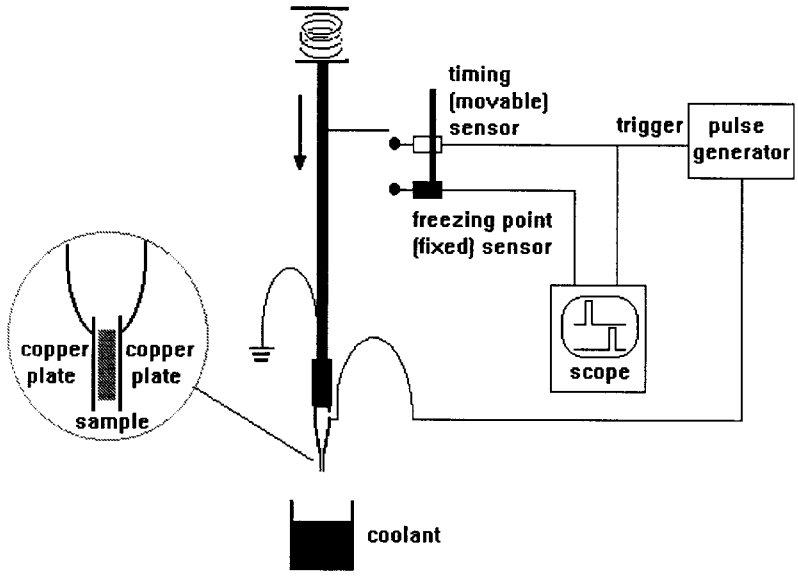

FIGURE 1 Schematic set-up for time-resolved pulsing and freezing of stratum corneum samples. The sample is propelled into the coolant quickly, using a spring and a plunger, to reduce freezing of the sample by crystalline ice. The timing sensors are infrared detectors, which are triggered by a bar attached to the plunger, one sensor is movable vertically (triggering the pulse) and the other is fixed (marking the time of freezing). The pulse and the fixed sensor output are recorded on the oscilloscope. Thus, the time between pulsing and freezing can be varied.

Areas of the sample, which contained vesicle aggregations, were photographed in the electron microscope and the negatives were analyzed. An aggregate of vesicles was defined as a group of five or more vesicles, which were touching or in close proximity to each other. The shape of vesicles was not an exclusive factor in this determination (Fig. 2).

RESULTS

Freeze-fractured samples of the stratum corneum consist of random fracture planes either along the membrane of the corneocyte or through the multilamellar lipid between them. Single, spherical, multi, or unilamellar vesicles of various sizes (mostly at the 0.1- to 2-μm range) were found in the lamellar lipid region or confined hydrated areas of the stratum corneum in the control (unpulsed) samples. (The frequency of appearance varied from sample to sample, but was generally very low. Multilamellarity was identified by the concentric layers of lipid of the vesicle, like those found in phospholipid multi-lamellar liposomes.) No vesicle aggregations were found. (Fig. 3 *A*).

When the sample was pulsed, vesicle aggregate structures were observed (Fig. 2). Aggregates vary from 0.6–30 μm across. Within these aggregates, some vesicles came into close contact with each other, similar to the aggregation and stacking of liposomes derived from stratum corneum lipids (Abraham et al., 1988). Many vesicles were shaped irregularly, although most were spherical. Aggregates were found in lipidic regions of the stratum corneum or surrounded by an aqueous background, which is likely to be water trapped between lipid multilayers.

Aggregations of vesicles were found as early as 0.5 ms (Fig. 3 *B*). The gaps between the vesicles were much smaller than the diameters of the vesicles themselves with many of the vesicles coming into contact with each other. At 12 ms, the size of the vesicles had decreased (Fig. 3 *C*). Many of the vesicles came into very close contact, becoming slightly oval in shape. After 5 s, the vesicle size had increased (Fig. 3 *D*). These vesicles persisted past 60 s (Fig. 3 *E*) but disappeared by 5 min (Fig. 3 *F*).

The morphological changes in the skin were quantified by four parameters: aggregate density, individual aggregate area, number of vesicles per aggregate, and vesicle diameter. Aggregate density was quantified by the total number of aggregates divided by the total replica area observed at each time point, typically ranging from 12–16 $\times$ 10^6 μm^2 (Fig. 4). Because aggregate formation was assumed to be a Poisson process, upper and lower confidence bounds were calculated and displayed in Fig. 4 (Johnson and Kotz, 1969). In order to obtain sufficient sampling for statistical analysis, data collection was concentrated on five time points, namely, 0.5 ms, 12 ms, 5 s, 60 s, and 5 min. Histograms were obtained in terms of the last three parameters and were displayed in three dimensional plots to illustrate the time evolution (see Figs. 5–7). The histograms were normalized by the total replica area observed for each sample, typically ranging from 0.5–3.6 $\times$ 10^6 μm^2. It was assumed that all replicas have the same ratio of usable to unusable areas, unusable being freeze damaged or contaminated areas, and fracture planes that were not along the stratum corneum.

Aggregate formations were found 0.5 ms after the pulse. The aggregate density steadily increased until it reaches an apex of 4 $\times$ 10^{-6} μm^{-2} at 5 s (Fig. 4). Past 5 s, the number of aggregates dropped, and by 5 min they had disappeared. The size distribution of the aggregates was skewed toward the smaller areas, 25–50 μm^2. These aggregates of small area increased in number and the distribution became more

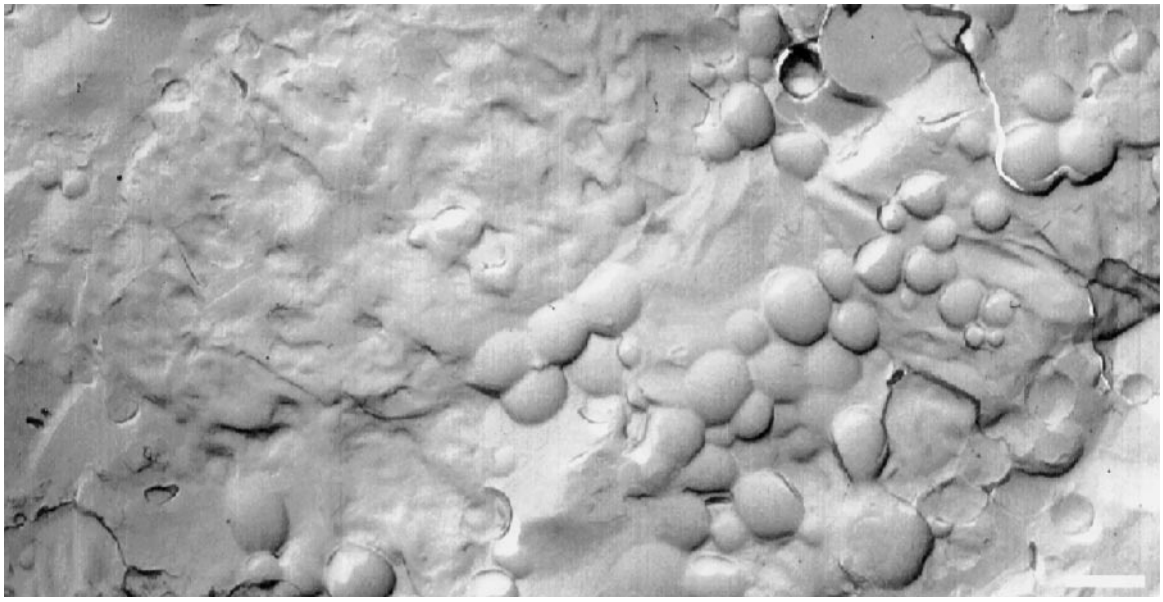

FIGURE 2 Freeze-fracture electron micrograph of a sample of stratum corneum, pulsed at 80 volts for 300 μs, and frozen 5 s after the pulse. The bar equals 1 μm.

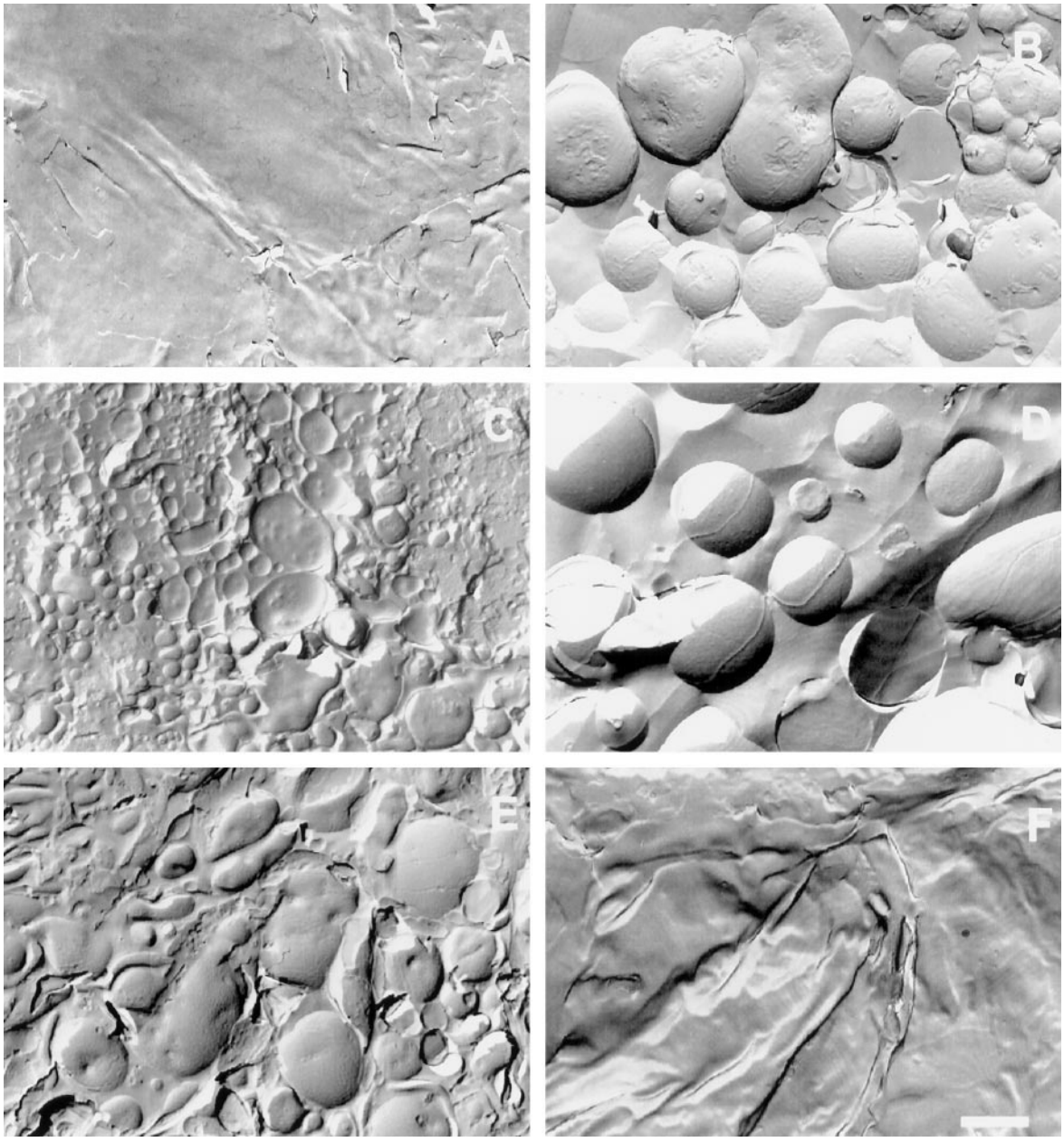

FIGURE 3 Freeze-fracture electron micrographs of (*A*) a control (unpulsed) sample of hydrated porcine stratum corneum and samples pulsed for 300 μs at 80 v, which were frozen (*B*) 480 μs after the pulse, (*C*) 12 ms after the pulse, (*D*) 5 s after the pulse, (*E*) 60 s after the pulse, and (*F*) 300 s after the pulse. The bar equals 1 μm.

skewed with time until 5 s, past which the number decreased rapidly (Fig. 5).

When plotted by the number of vesicles per aggregate, the density distribution was flat at 0.5 ms, but by 12 ms it was skewed to the lower number because of an increase in aggregates containing 10–20 vesicles. The trend continued at the 5-s time point, but by 60 s the number of aggregates had decreased considerably (Fig. 6).

The vesicle size distribution was different from the aggregation size distribution. The total number of vesicles for each time point was approximately the same. At 0.5 ms, the distribution of vesicle size was centered around 1 μm in diameter. At 12 ms the distribution became skewed toward 0.5 μm. At longer time points, the distribution resembled that of 0.5 ms (Fig. 7).

To investigate if vesicle formation is related to sample heating caused by the pulse, the stratum corneum was heated to 65°C for 15 s prior to freezing without pulse application. The heat treated samples were observed to contain vesicle aggregates (Fig. 8). The aggregate areas were 1.8 μm^2 (0.6–4.1 μm^2) on the average and the number of vesicles per aggregate ranged from 30–60 (an average of 49). No histogram plots were made for these two parameters because the number of aggregates was too small to make

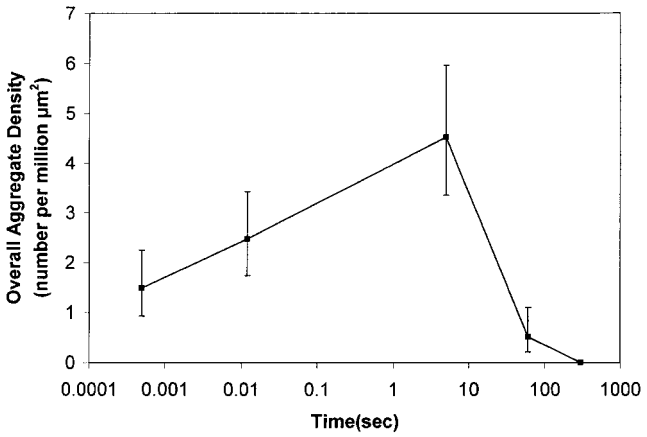

FIGURE 4 Plot of overall aggregate density. The total number of aggregates divided by the total observed replica area is plotted against time after pulse application (logarithmic scale). The number of samples used per time point ranged from 7–8.

such analysis useful. The vesicle diameter distribution was skewed to the left, ~0.1 μm (Fig. 9), although the vesicle diameters in Fig. 8 were somewhat larger than this (>200 nm). A high number of small vesicles (<100 nm) was observed. The average aggregate density was 0.27×10^{-6} μm^{-2}, slightly lower than that of samples frozen 60 s after pulsing.

DISCUSSION

There have been many electrical and molecular transport measurements of the electroporation of the skin since the first report of the application of this technique to transdermal delivery. Based on these measurements, several models have been proposed (Chizmadzhev et al., 1995, Edwards et al., 1995, Pawlowski et al., 1999). However, little is known about the structural changes during the electroporation process and the subsequent recovery period. There has not been a report on the direct visualization of the structural changes, at the electron microscopic level, of the stratum corneum during and after high voltage pulse application. Knowledge of the pulse-induced structural changes of the stratum corneum is paramount to understanding and optimizing skin electroporation for transdermal delivery. Pliquett et al. (1996b) reported an observation of localized transport regions of charged fluorescent dyes through the stratum corneum mounted between flow-through chambers. These long-lasting localized transport regions reach diameters of 40–80 μm. The correlation between the timing of the appearance of these regions to that of the measured drop of the electrical resistance of the samples has yet to be determined.

The goal of our study is to examine ultrastructural changes occurring immediately after the applied electroporating pulse. The typical feature of freeze-fractured stratum corneum is a fracture plane passing through intercellular lipid multilayers (Fig. 3 *A*). The aqueous background of the fracture plane is rarely seen. Unpulsed, hydrated control samples showed occasional single, multilamellar or unilamellar vesicles. Vesicle formation in unpulsed samples has also been observed by Bouwstra's group (Van Hal et al., 1996), in which trypsinized stratum corneum exposed to intense hydration (48-h incubation in buffer solution) was freeze fractured. Unilamellar vesicles and, rarely, vesicle aggregates were observed. Stratum corneum lipids extracted by chloroform:methanol solutions readily form unilamellar vesicles in aqueous solutions and form aggregates in the presence of acylceramides (Abraham et al., 1988). Because dry samples have not been observed by freeze-fracture electron microscopy, it is not known whether vesicle formation is entirely a result of hydration. Variable hydration levels probably contributed a great deal to the variability in reported results. It is not known whether vesicles form in hydrated skin in vivo. Heat may also be an effector in vesicle formation. The harsh treatment of the sample during the heat stripping may effect the stratum corneum lipids in an irreversible manner. This may be caused by the irreversible phase transition at 60°C of the pig stratum corneum lipids (Potts and Francoeur, 1992), changing their physical

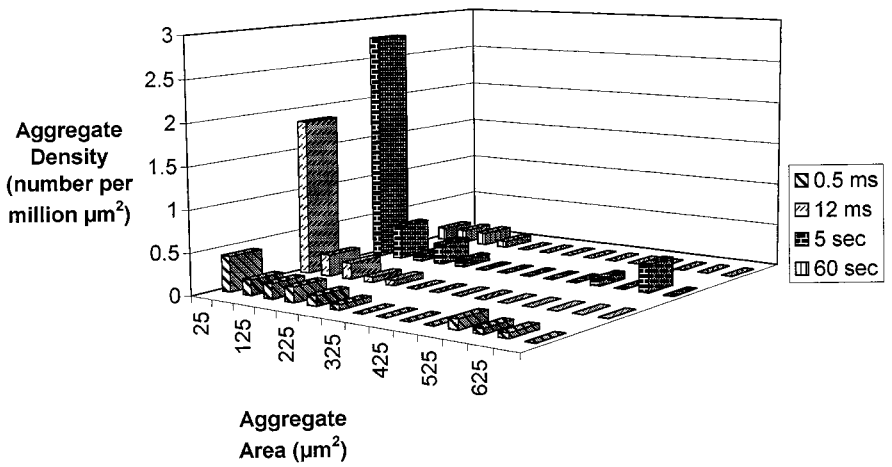

FIGURE 5 Three-dimensional histogram analysis of the aggregate density according to the aggregate size and its time evolution. The number of aggregates divided by the total observed area per time point is plotted against aggregate area.

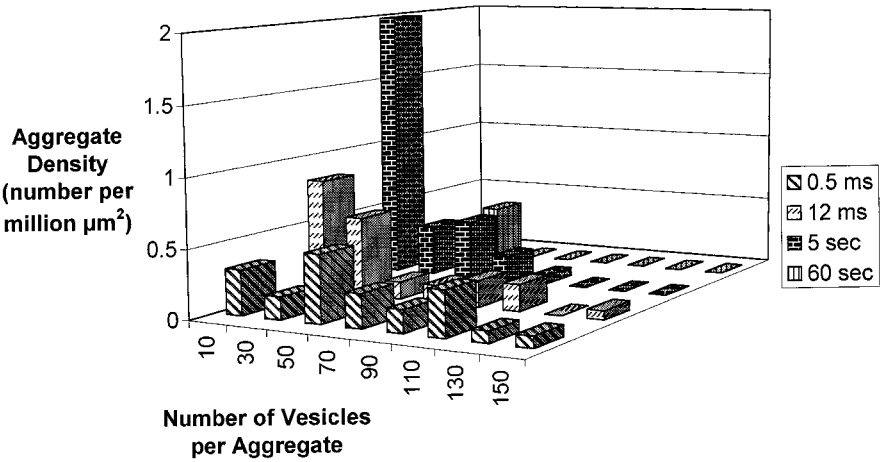

FIGURE 6 Three-dimensional histogram analysis of the aggregate density according to the number of vesicles per aggregate and its time evolution. The number of aggregates divided by the total observed area per time point is plotted against vesicle number.

properties and possibly making them more amenable to vesicle formation.

The main feature distinguishing pulsed samples from control samples is the density of vesicle aggregations. In pulsed samples, aggregated vesicles were frequently observed (Figs. 2 and 3 *B-E*). The aggregate density steadily increases from 0.5 ms after the pulse to seconds later (Fig. 4), implying that most of these structures form after the pulse and may not be directly responsible for the transient electric permeability decreases of the skin seen during the pulse (Gallo et al., 1997; Pliquett et al., 1995). These structures probably represent reactions of the skin to the pulse and not the original electrical resistance breakdown of the stratum corneum bilayers during the pulse. The density of aggregates increases, but the aggregate size and vesicles per aggregate decrease with time until 5 s after the pulse when the number of aggregates also falls and reaches zero in 5 min (Figs. 4–6). At the same time, the peak of vesicle size distribution shifts from 1 μm at 0.5 ms to $<$0.5 μm at 12 ms and then back to 1 μm at 5 s (Fig. 7). It is possible that we are observing two processes. These large vesicles seen at 0.5 ms may fuse into the lipid lamellae of the stratum corneum or break up into smaller vesicles in the first few milliseconds. The smaller vesicles seen at 12 milliseconds may eventually fuse together to form larger vesicles or fuse back into the lipid lamellae in the ensuing seconds to minutes. Differences in vesicle stability could account for variation in relaxation times.

The vesicle aggregates eventually disappear minutes after the pulse (Figs. 3 *E* and 4). The timing of aggregate appearance seems to correspond well to the electrical resistance recovery of heat-stripped stratum corneum in flow-through chambers in which most of the initial resistance is regained in tens of seconds to minutes (Pliquett et al., 1995). This may suggest that the aggregates are correlated with the recovery of the stratum corneum from the electrical pulse. Postpulse resistance measurements in our samples could not be made because of a change in the interfacial resistance between the skin and the copper electrode presumably because of an electrochemical reaction.

Based on the ultrastructural observation and electrical measurements, we may speculate that areas of high current density or localized electrical breakdown may be responsible for the initial disturbances. The initial bilayer disturbance by the pulse, coupled with an environment change such as water penetration, could initiate the formation of aggregates of vesicles. Large aggregates begin to break up with time. The mechanism of this process may be related to the diffusion of water in the stratum corneum. The lateral diffusion constant for water in the stratum corneum is 1.9 $\times$

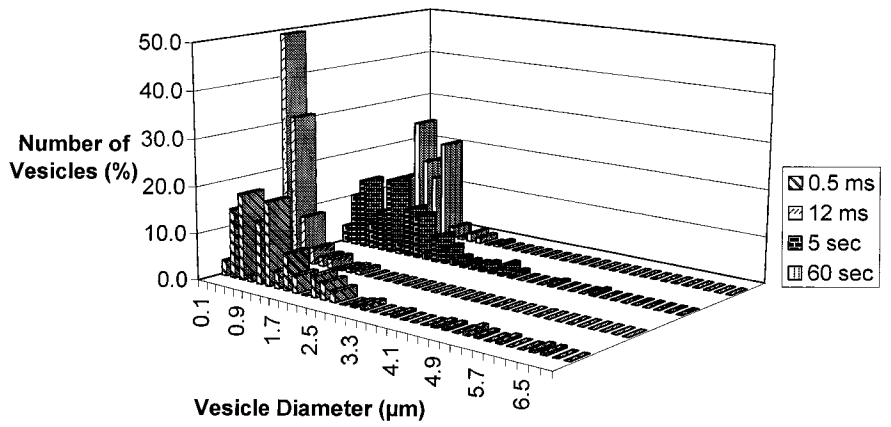

FIGURE 7 Three-dimensional histogram analysis of the number of vesicles according to the vesicle diameter and its time evolution. The percentage of the total number of vesicles per time point is plotted against vesicle diameter.

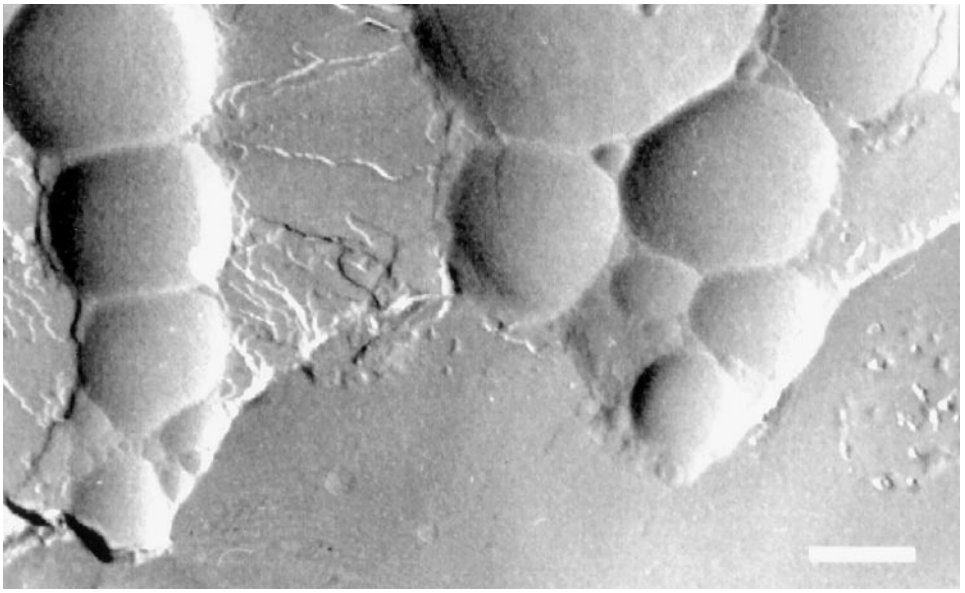

FIGURE 8 Freeze-fracture electron micrograph of a stratum corneum sample heated for 15 s at 65°C and frozen immediately. The bar equals 200 nm.

10^{-5} cm^2/s (Johnson et al., 1997), and if one assumes to have a thin layer of solution sandwiched between a homogenous skin matrix, the diffusion coefficient is equal to one half the mean-square displacement of water per unit time. This corresponds to an expansion velocity of ~ 1 μm/ms. If one assumes that the aggregates and water pools are dispersed across the skin every several micrometers or so from each other, then this time scale matches that of the breaking up of large aggregates into smaller ones (Figs. 5 and 6), which result in the increase in the aggregate density (Fig. 4). Fusion among these metastable vesicles into giant liposomes and between liposomes and lipid lamellae of the stratum corneum would eventually restore the stratum corneum to its initial state. The competition between these two types of fusion processes could be responsible for the reverse shift of the vesicle size distribution peak, as shown in Fig. 7.

Formation of vesicles from relatively dry lipid lamellae of the stratum corneum requires external energy to be added to the system. This energy is imparted to the lamellae either by the dielectric breakdown of the bilayers during the pulse and/or in the form of local joule heating at the permeabilized sites by the pulse-induced current. We have shown that uniformly heated samples also elicit localized aggregates of vesicles (Fig. 8). Because of the inhomogeneity of the stratum corneum, some defect areas may be compromised first, leading to the localization of vesicles. Heat-created pores may also create localized structures (Shillcock and Seifert, 1998). Comparisons can be made between the energy necessary to heat the sample to 65°C and the energy of

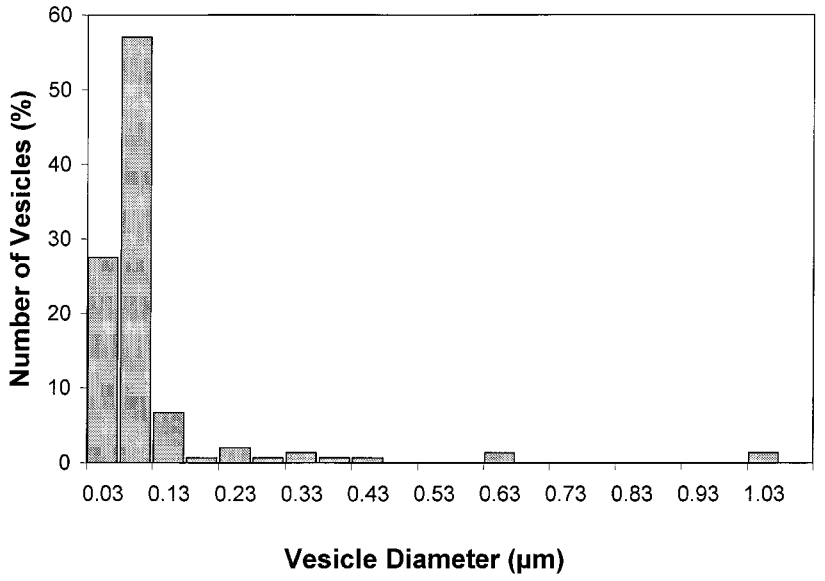

FIGURE 9 Histogram analysis of the number of vesicles according to the vesicle diameter for the heated sample. The percentage of the total number of vesicles is plotted against vesicle diameter.

an 80-volt pulse dissipated by joule heating. Considering a 1-mg sample and the heat capacity of water (4.2 J/g*°C), the enthalpy to raise the sample from 25 to 65°C is 170 mJ. Distributed across the sample diameter of ~1.5 mm and a thickness of ~20 μm, the energy density is 5 nJ/μm^3. The energy dissipated by an 80-volt, 300-μs pulse over a 50-kohm resistance is ~40 μJ, or 1 pJ/μm^3 dispersed over the whole sample. Electroporation at 80 volts is likely to cause at least an order of magnitude drop in resistance, increasing the total energy to 400 μJ. If one assumes this energy to be concentrated among ~70 aggregates (18×10^6 μm^2 (total sample area) $\times 4 \times 10^{-6}$ μm^{-2} (density at 5 s)) with areas of ~25 μm^2 (average aggregate area at 5 s) and a stratum corneum thicknesses of 20 μm, the energy density at these aggregation sites is 11 nJ/μm^3. Thus the energy density created from our heat treatment could be on the same order of magnitude as that of the pulse. The aggregates seen in the 80-volt pulsed sample, though, were larger and appeared much more frequently than the heated sample (Figs. 8 and 9). It may be that the initial membrane disturbance takes the form of an electropore, which is estimated to be nanometers in diameter (Chizmadzhev et al., 1995). The energy density caused by electroporation at these initial sites could be many orders of magnitude higher because of this restriction in area, although pore density must be known to make this calculation. No initial electropores are observed in these samples, possibly because they are too small and transient to be seen. Also, it has been reported that cuvette systems with aluminum electrodes may exhibit postpulse heating because of electrochemical reactions on the electrode surface (Pliquett et al., 1996a). Although temperature differentials of 40° can occur for seconds after pulsing, these effects are greatly dependent on the conductivity of the medium and the size and composition of the electrode. It seems evident from these calculations that bulk (joule and electrochemical) heating alone is not likely to cause the response seen in the skin after the pulse, although at the site of initial breakdown, high current density may concentrate the heating and be a more likely effector.

The relationship between the transient permeability of the skin and the formation of aggregates is still unclear. Although this data is indicative of some recovery process and correspond well with electrical recovery results in other heat-stripped systems (Pliquett et al., 1995), there is no data on the electrical resistance recovery of this particular system. Studies of the aggregate density at the 5-s postpulse time point show a similar voltage dependency (results not shown) as that for the electric permeabilization of the full thickness of skin during a single pulse (Gallo et al., 1997). At this point, though, the similarity of these data is merely suggestive.

Our study is restricted to the response from a single pulse. It is not clear what effect multiple pulses will have on vesicle structures. Long-term permeabilization trends have been seen as a result of multiple pulsing with electrical recovery taking minutes to hours or remaining incomplete (Pliquett et al., 1995, Gallo et al., 1997). Aggregates may not recover or perhaps the skin becomes saturated with water because of the breakdown of the barrier function, needing minutes to hours to dehydrate, and thus preventing recovery. Additional structural studies need to be conducted to make any conclusions.

Some similarities exist between the aggregates found in this study and in the localized transport regions (LTR) found in flow-through permeation chamber studies (Pliquett et al., 1996b). Both appear shortly after the pulse (the temporal resolution of the fluorescent imaging apparatus was ~0.5 s) and lasted minutes to hours afterwards. Aggregates sizes vary from 1–30 μm in diameter, somewhat smaller than the LTR, which range from 40–80 μm in diameter. This could be caused by diffusion of the dye and the use of more stringent-pulsing conditions. The fractional area of the aggregates, calculated as the summed aggregate area divided by the total sampled area ranged from 0.05–0.5%, whereas LTR ranged from 0.02–0.05% for 80-volt pulses. This discrepancy may be explained by the difference in resolution of the two imaging modalities. Because of the striking similarities between these two findings, there is added support to the hypothesis that the formation of these aggregate structures is quite relevant to transdermal drug delivery. How these structures are related, if at all, to the elusive electropore and how their formation can be optimized for drug delivery needs additional study. Whether aggregates of vesicles form in full thickness skin in vivo as a result of the pulse still remains to be seen. In any case, this ultrastructural study provides a basis for elucidating the mechanism of skin electroporation.

Supported by Grant GM 55864 from the National Institutes of Health. We thank Dr. John Canty of the Department of Medicine at SUNY (Buffalo, NY) who supplied some of the porcine skin for this project. Mr. Brian Chow and Mr. George Potienko fabricated the time-resolved freezing device. Statistical analysis was performed with the help of Dr. William Greco, Biostatistics Facility, which is supported by the CCSR Grant CA 16056 from the National Cancer Institute.

REFERENCES

Abraham, W., P. W. Wertz, and D. T. Downing. 1988. Effect of epidermal acylglucosylceramides on the morphology of liposomes prepared from stratum corneum lipids. *Biochem. Biophys. Acta.* 939:403–408.

Bommannan, D. B., J. Tamada, L. Leung, and R. O. Potts. 1994. Effect of electroporation on transdermal iontophoretic delivery of luteinizing hormone releasing hormone (LHRH) in vitro. *Pharm. Res.* 11:1809–1814.

Bouwstra, J. A., G. S. Gooris, A. Weerheim, J. Kempenaar, and M. Ponec. 1995. Characterization of stratum corneum structure in reconstructed epidermis by X-ray diffraction. *J. Lipid Res.* 36:496–504.

Bronaugh, R. L., and H. I. Maibach. 1989. *In* Percutaneous Absorption, Mechanisms — Methodology — Drug Delivery. Marcel Dekker, New York.

Chang, D. C., B. M. Chassy, J. A. Saunders, and A. E. Sowers. 1992. *In* Handbook of Electroporation and Electrofusion. Academic Press, New York.

Chang, D. C., and T. Reese. 1990. Changes in membrane structure induced by electroporation as revealed by rapid-freezing electron microscopy. *Biophys. J.* 58:1–12.

Chizmadzhev, Y., V. Zarnytsin, J. C. Weaver, and R. O. Potts. 1995. Mechanism of electroinduced ionic species transport through a multi lamellar lipid system. *Biophys. J.* 68:749–765.

Chizmadzhev, Y. A., A. V. Indenbom, P. I. Kuzmin, S. V. Galichencko, J. C. Weaver, and R. O. Potts. 1998. Electrical properties of skin at moderate voltages: contribution of appendageal macropores. *Biophys. J.* 74:843–856.

Edwards, D. A., M. R. Prausnitz, R. Langer, and J. C. Weaver. 1995. Analysis of enhanced transdermal transport by skin electroporation. *J Control. Release.* 34:211–221.

Ferry, L., G. Argentieri, and D. Lochner. 1995. The comparative histology of porcine and guinea pig skin with respect to iontophoretic drug delivery. *Pharm. Acta Helv.* 70:43–56.

Gallo, S. A., A. R. Oseroff, P. G. Johnson, and S. W. Hui. 1997. Characterization of electric-pulse-induced permeabilization of porcine skin uing surface electrodes. *Biophys. J.* 72:2805–2811.

Hadgraft, J., and R. H. Guy. 1989. *In* Transdermal Drug Delivery, Developmental Issues, and Research Initiatives. Marcel Dekker, New York.

Johnson, M. E., D. Blankschtein, and R. Langer. 1997. Evaluation of solute permeation through the stratum corneum: lateral bilayer diffusion as the primary transport mechanism. *J. Pharm. Sci.* 86:1162–1172.

Johnson, N. L., and S. D. Kotz. 1969. *In* S. D. Discrete Distributions. John Wiley and Sons, New York.

Johnson, P. G., S. A. Gallo, S. W. Hui, and A. R. Oseroff. 1998. A pulsed electric field enhances cutaneous delivery of methylene blue in excised full-thickness porcine skin. *J. Invest. Dermatol.* 111:457–463.

Madison, K. C., D. C. Swartzendruber, P. W. Wertz, and D. T. Downing. 1987. Presence of intact intercellular lipid lamella in the upper layers of the stratum corneum. *J. Invest. Derm.* 88:714–718.

Pawlowski, P., S. A. Gallo, P. G. Johnson, and S. W. Hui. 1999. Electrorheological modelling of the permeabilization of the stratum corneum: theory and experiment. *Biophys. J.* 75:2721–2731.

Pliquett U., E. A. Gift, and J. C. Weaver. 1996a. Determination of the electric field and anomalous heating caused by exponential pulses with aluminum electrodes in electroporation experiments. *Bioelectrochem. Bioenerg.* 39:39–53.

Pliquett, U., R. Langer, and J. C. Weaver. 1995. Changes in the passive electrical properties of human stratum corneum due to electroporation. *Biochim. Biophys. Acta.* 1239:111–121.

Pliquett, U. F., T. E. Zewert, T. Chen, R. Langer, and J. C. Weaver. 1996b. Imaging of fluorescent molecule and small ion transport through human stratum corneum during high voltage pulsing — localized transport regions are involved. *Biophys. Chem.* 58:185–204.

Potts, R. O., and M. L. Francoeur. 1992. Physical methods for studying stratum corneum lipids. *Semin. Dermatol.* 11:129–138.

Prausnitz, M., V. Bose, R. Langer, and J. C. Weaver. 1993. Electroporation of mammalian skin: a mechanism to enhance transdermal drug delivery. *Proc. Natl. Acad. Sci. USA*. 90:10504–10508.

Schurer, N. J., and P. M. Elias. 1992. The biochemistry and function of stratum corneum lipids. *Adv. Lipid Res.* 24:27–56.

Shillcock, J. C., and U. Seifert. 1998. Thermally induced proliferation of pores in a model fluid membrane. *Biophys. J.* 74:1754–1766.

Stenger, D. A., and S. W. Hui. 1986. Kinetics of ultrastructural changes during electrically induced fusion of human erythrocytes. *J. Membr. Biol.* 93:43–53.

Van Hal, D. A., E. Jeremiasse, H. E. Junginger, F. Spies, and J. A. Bouwstra. 1996. Structure of fully hydrated human stratum corneum: a freeze-fracture electron microscopy study. *Soc. Invest. Dermatol.* 106: 89–95.

Vanbever, R., and V. Preat. 1995. Factors affecting transdermal delivery of metoprolol by electroporation. *Bioelectrochem. Bioenerg.* 38:223–228.

Yamamoto, T. 1977. Electrical properties of the epidermal stratum corneum. *Med. Biol. Eng.* 14:151–158.

Zewert, T. E., U. F. Pliquett, R. Langer, and J. C. Weaver. 1995. Transdermal transport of DNA antisense oligonucleotides by electroporation. *Biochem. Biophys. Res. Commun.* 212:286–292.